Science
AAAS

Supplementary Materials for

The cryosphere beyond a planetary safe operating space

Bo Su *et al*.

Corresponding authors: Bo Su, bo.su@su.se; Deliang Chen, deliangchen@tsinghua.edu.cn; Lan Wang-Erlandsson, lan.wang@su.se

DOI: 10.1126/science.aef5636

The PDF file includes:

Materials and Methods
Supplementary Text
Figs. S1 to S3
Tables S1 to S6
References

Materials and Methods

Evaluation and selection of cryosphere control variables

According to the definition and purpose of the PB framework, any boundary must be grounded in well-understood control–response relationships, have demonstrable impacts on Earth system stability, and exhibit scalable mechanisms through which regional perturbations can propagate to the global level(*90*). Proposed boundaries should also be measurable, representative, understandable, operational, and unique, ensuring both scientific robustness and policy relevance(*1*). Following these principles, we established four criteria for selecting cryosphere control variables: *i)* importance for maintaining Holocene-like conditions, *ii)* susceptibility to anthropogenic perturbation, *iii*) universality and uniqueness, and *iv)* measurability.

Candidate variables were identified through literature review, expert elicitation, iterative discussion, and consensus-based workshops. We first assessed the functional roles, similarities, and differences among cryosphere elements (Table S1), classifying the cryosphere into five subsystems: land ice (ice sheets and mountain glaciers), sea ice, snow cover, permafrost, and atmospheric ice. Potential control variable candidates were then compiled from the literature and expert input (Table S2). Applying the four criteria, experts scored each candidate, and consensus was reached through subsequent discussions.

Ultimately, we selected four cryosphere control variables—land ice volume, sea ice area, snow cover area, and permafrost temperature—to represent the dominant cryosphere–Earth system interactions (Table S3). Components with negligible global influence (e.g., river ice, lake ice, icebergs) were excluded. However, changes in lake ice and river ice are already having a profound impact on many mountain communities. Ice shelves were considered together with ice sheets, and atmospheric ice was excluded because it is neither unique to the cryosphere.

Land ice volume captures the total frozen water storage of the planet and directly reflects net gains or losses from ice sheets and glaciers(*29*). It serves as a robust indicator of land ice stability, anthropogenic influence, and planetary-scale impacts on sea level, climate, and polar and high-mountain ecosystems(*11*). This variable is well-constrained through land ice models, in situ observations, and satellite missions such as GRACE (Gravity Recovery and Climate Experiment)(*11*), providing a quantifiable and sensitive measure of cryospheric health.

Sea ice area quantifies the total surface coverage of sea ice in the Arctic and Southern Ocean(*11*). It is a key indicator of cryospheric stability, directly linked to albedo feedbacks, energy balance, and polar marine ecosystem health(*91*). Sea ice area is one of the best-observed cryospheric variables, with high-quality records derived from satellite passive microwave sensors and coupled sea ice models(*53*), allowing precise detection of long-term trends and thresholds.

Snow cover area measures the spatial extent of global snow cover, a critical determinant of planetary albedo, heat exchange, and atmospheric circulation(*61*). Stable snow cover during the Holocene helped regulate global energy balance and hydrological and carbon cycles across biomes(*92*). Anthropogenic warming has driven widespread snow cover decline, particularly in the Northern Hemisphere. Compared with variables such as snow depth or snow-water equivalent, snow cover area is more directly measurable and globally representative. Advances in remote sensing (e.g., MODIS, Landsat), ground-based observations, and Earth system modeling now enable precise, continuous monitoring at global scales(*11*).

Permafrost temperature represents the thermal state of frozen ground and integrates the effects of atmospheric warming, soil properties, energy flux changes, and local climate variability(*11*). Warming permafrost leads to greenhouse gas emissions (CO_2, CH_4), ground instability, and ecosystem collapse, all of which amplify global climate change(*78*, *93*). Mean permafrost temperature is a widely used and measurable indicator, routinely monitored through land process models and high-resolution observations(*11*), making it suitable for tracking systemic risk and early warning of tipping behavior. While we retain permafrost temperature as the primary control variable because of its superior performance according to the control variable selection criteria, the permafrost area was also chosen as a supplementary variable to support permafrost boundary transgression assessment. Permafrost temperature and permafrost area exhibit markedly different response characteristics. The latter often exhibits a substantially delayed response, reflecting the long timescales required for thaw to propagate through deep ground layers(*11*).

Together, these four control variables capture the essential dimensions of cryosphere–Earth system coupling and provide a scientifically robust foundation for delineating a SOS for the cryosphere.

Formulation of cryosphere control variables

For land ice, the control variable is defined as the total ice volume, encompassing all land-based ice masses, including mountain glaciers, the Greenland Ice Sheet, and the Antarctic Ice Sheet. This formulation provides several advantages. First, total ice volume offers a direct and comprehensive measure of global land ice storage(*91*), reflecting its overall stability and health. Second, because changes in ice mass directly alter frozen water storage and sea level, this variable enables robust assessment of the land ice contribution to global sea level rise and freshwater availability(*94*, *95*). Third, it captures scalable mechanisms by which regional ice loss aggregates to produce planetary-scale impacts. Finally, substantial and accelerating reductions in land ice volume serve as early warning signals of approaching tipping points or irreversible melting(*34*), providing valuable information for policy and risk management.

For sea ice, the control variable is defined as the total annual-mean sea ice area from both the Arctic and Antarctic. Likewise, the control variable for snow cover is defined as the annual-mean global snow-covered area. Using annual means provides a stable and policy-relevant indicator of long-term cryosphere trends, minimizing the influence of seasonal fluctuations and short-term variability.

For permafrost, the control variable is formulated as the mean annual ground temperature (MAGT), averaged over the spatial domain of the maximum preindustrial permafrost region (1850-1899). The MAGT is measured at the depth of minimum or zero annual thermal amplitude for each grid cell, with permafrost area defined as those exhibiting negative MAGT(*33*). This formulation offers an integrated and temporally stable measure of permafrost thermal state, capturing both gradual warming and the potential onset of tipping behavior leading to irreversible thaw.

Quantification of Holocene baseline departure

We quantified the Holocene baseline departure for each cryosphere control variable using reconstructed datasets, multi-model simulations, and observational records. Where available, the full Holocene is used to define baseline variability; otherwise, mid-Holocene and pre-industrial conditions are applied in this provisional assessment. The mid-Holocene experiment is not intended to represent the entire Holocene variability, but rather to provide an approximate

reference state for evaluating departures from Holocene-like conditions. Existing paleoclimate evidence generally suggests that the mid-Holocene was characterized by reduced Northern Hemisphere sea ice, reduced snow cover(*96*), and warmer permafrost conditions across the entire Holocene(*97*), although the magnitude and timing of these changes varied regionally. Thus, the selected period captures a lower bound of Holocene variability but cannot fully characterize its entire range(*26*). The early industrial period (1850–1899), which is widely regarded as largely unaffected by anthropogenic forcing, serves as a standard baseline in climate and Earth system assessments(*11*). As our mid-Holocene analysis of sea ice, snow cover, and permafrost relies on a single model and experiment, the CESM2 Earth System Model (700 years simulation, ~6,000 years BP)—we adopt the early-industrial period as our primary baseline, drawing on a multi-model ensemble to reduce uncertainties.

Land ice

The time series of total and component land ice volumes were reconstructed from their estimated present-day volumes and the corresponding mass balance (sea-level equivalent) variability(*28*, *29*). The assessment of land ice mass changes draws primarily on two reconstructed time series. The first spans the entire Holocene (11,700 years ago to 1950 CE)(*28*), while the second provides multi-method estimates of land ice mass change from 1900 to 2018(*29*). Mountain glacier mass changes are based on (1) a global glacier model reconstruction for the twentieth century(*98*), and (2) in situ glaciological and geodetic observations covering 1960–2018(*99*). Estimates for the Greenland Ice Sheet derive from (1) a mass-balance reconstruction for 1900–2003(*100*), (2) input–output estimates for 1972–2003(*101*), and (3) multi-method assessments for 1993–2003(*94*), and the GRACE-based estimates for 2003–2018(*29*). For the Antarctic Ice Sheet, a small pre-1993 contribution (0.05 ± 0.04 mm yr^{-1}) was assumed(*102*), while mass changes for 1993–2003 were taken from multi-method assessments(*94*, *103*), and changes for 2003–2018 were estimated based on GRACE observation(*29*). The 2010 global ice volumes are assumed as follows: mountain glaciers (excluding Greenland and Antarctic peripheries), 0.088×10^6 Gt (0.096×10^6 km^3)(*30*); Antarctica, 24.794×10^6 Gt (27.0465×10^6 km^3)(*32*), and peripheral glaciers (46.5×10^3 km^3)(*30*); and Greenland, 2.756×10^6 Gt (3.006×10^6 km^3), including the ice sheet (2.99×10^6 km^3)(*31*) and peripheral glaciers (15.7×10^3 km^3)(*30*). Ice density was assumed to be 0.9167 Gt km^{-3}, and 362.5 Gt of ice was taken as equivalent to 1 mm of global mean sea-level rise(*11*). Committed ice loss is based on Zekollari et al. (2025)(*75*) for mountain glaciers, Box et al., (2022) for Greenland ice sheet(*76*), as well as DeConto et al., (2021) and Klose et al., (2024) for Antarctic ice(*45*, *77*). The uncertainty in reconstructed land-ice volume arises from the combined propagation of uncertainties associated with historical ice-change reconstructions, recent ice-volume estimates, and committed ice-loss projections. Uncertainty in the reconstructed relative ice changes primarily reflects observational limitations, structural differences between sea-level and ice-sheet reconstructions, and uncertainties in glacial isostatic adjustment (GIA), together with contributions from glacier and ice-sheet mass-balance estimates, thermosteric expansion, terrestrial water storage changes, and vertical land-motion corrections(*28*, *29*). Additional uncertainty originates from the 2010 baseline ice volume used to convert relative changes into absolute ice volume, which is mainly affected by the limited availability of observational constraints(*30–32*). Furthermore, uncertainty in committed ice loss is associated with structural differences among models, inconsistencies among multi-source datasets, and systematic errors in model formulations and calculation procedures(*75–77*). Collectively, these uncertainties propagate through the reconstruction process and influence the magnitude of the estimated land-ice volume, while the overall long-term evolution remains robust across datasets and model ensembles.

Sea ice

Because continuous Holocene sea ice data are unavailable, we assessed baseline departure of sea ice area using model-based reconstructions. Monthly sea ice coverage was obtained from the mid-Holocene experiment (700 years beginning ~6,000 years ago) and historical (1850–2014) simulations of the CESM2 Earth System Model (CMIP6). CESM2 couples atmospheric (CAM6/WACCM6), oceanic (POP2), sea ice (CICE5), land (CLM5), and ice sheet (CISM2) components(*104*). Its sea ice simulations are broadly consistent with satellite observations for 1990–2024 from the National Snow and Ice Data Center (NSIDC). For cross-validation, we also used ISIMIP3b ocean input data (1850–2014) (Table S4), remapped to a 1° × 1° grid and derived from four CMIP6 global climate models (GFDL-ESM4, IPSL-CM6A-LR, MPI-ESM1-2-HR, and UKESM1-0-LL). The ISIMIP ensemble captures observed trends in sea ice decline, albeit with inter-model spread.

The uncertainty in simulated sea ice primarily arises from inter-model structural differences, internal climate variability, and limitations in the representation of key sea ice–ocean–atmosphere coupled processes within CMIP6-class models(*105*). In particular, divergence among simulations reflects differences in sea ice thermodynamic schemes, including melt–growth processes, snow–ice conversion, and parameterizations of ice albedo feedback(*106*).

Snow cover

The baseline departure of snow cover area was estimated using three complementary monthly datasets: (1) CESM2 mid-Holocene and historical simulations, analogous to the sea ice and permafrost assessments; (2) historical snow cover data from 13 CMIP6 Earth system models (nominal 100 km resolution; Table S6); and (3) ERA5-Land monthly snow cover data (1950–2024; 0.1° resolution)(*107*). The mid-Holocene (~6 ka BP; 700-year period) and pre-industrial (1850–1899) intervals were used as baseline reference periods based on CESM2 and CMIP6 multi-model means, respectively. Uncertainty in simulated snow-cover area primarily arises from inter-model structural differences, particularly in the representation of snowfall partitioning, snow accumulation and ablation, snow-albedo feedbacks, and vegetation–snow interactions(*92*, *105*). Such uncertainty mainly affects the magnitude of projected changes, whereas the direction of the long-term trend remains robust across the CMIP6 ensemble.

Permafrost

Baseline departures in permafrost mean annual ground temperature (MAGT) are estimated from CESM2 mid-Holocene and historical simulations (1.25° spatial resolution) and the ISIMIP3b permafrost output dataset (0.5° resolution; 42 m depth). The ISIMIP3b simulations employ the ELM-ECA land component of the E3SM model, forced by bias-corrected outputs from five CMIP6 models (GFDL-ESM4, IPSL-CM6A-LR, MPI-ESM1-2-HR, MRI-ESM2-0, and UKESM1-0-LL) (Table S5). The mid-Holocene (~6 ka BP) and pre-industrial (1850–1899) periods were used as baseline references based on CESM2 and ISIMIP multi-model means, respectively. The uncertainty in simulated permafrost dynamics primarily arises from inter-model structural differences, internal climate variability, and limitations in process representation. In particular, inter-model divergence reflects differences in the parameterization of soil thermal and hydrological processes, phase-change physics, and unfrozen water content, as well as strong sensitivity to snow insulation effects that regulate the surface energy balance (*108*, *109*). Collectively, these factors contribute to substantial ensemble spread in simulated permafrost evolution across mid-Holocene and historical periods. Nevertheless, the ensemble simulations still capture the first-order patterns of permafrost variability.

Supplementary Text

Earth System Functions of the Cryosphere SOS

We first identify the scope of an SOS of the cryosphere, focusing on the effect of the cryosphere on the Earth system resilience and fundamental conditions for human habitability on a planetary scale by following the planetary boundaries (PB) framework. The cryosphere components play critical roles in the functioning and stability of the Earth system through mediation of the energy, water, and carbon balance, which are fundamentally inextricable from other parts of the Earth system underlying the existing PB(*1*, *20*). In particular, the functional cryosphere changes can significantly affect the two so-called "core" boundaries, i.e., climate change and biosphere integrity(*2*, *21*), which constitute the aggregate manifestation of the main interactions among all the other boundaries, and have a decisive impact on the Earth system stability. Meanwhile, nonlinear transitions or regime shifts within the cryosphere also influence other non-"core" boundaries, especially for freshwater change PB. Building on existing scientific evidence and reports (Table S1), here we classify the Earth system functions of the cryosphere into three major categories: (1) cryo-climatic regulation, (2) cryo-ecological regulation, and (3) cryo-hydrological regulation.

Cryo-climatic regulation

The cryosphere exerts an important influence on Earth system resilience by regulating the Earth's climate based on its special nature and properties, complex structures and processes. Among others, snow and ice can directly reflect a large fraction of solar radiation back into space owing to their inherently high albedo, hence regulating the quantity of solar energy absorbed by land and oceans(*110, 111*). The cryosphere, especially glaciers, ice sheets, sea ice, and permafrost, acts as Earth's massive heat storage system—the second largest component of the climate system (after the ocean), which acts as a crucial buffer capacity for preventing global warming(*112*). Additionally, snow and ice are excellent thermal insulators characterized by low thermal conductivity, allowing them to serve as a buffer against temperature changes(*113*). Huge latent heat exchange in the cryosphere is also a fundamental process that underpins the climate system(*114*). The cryosphere's latent heat dynamics stabilize global temperatures near the ice-water transition point (~0°C), a balance critical for maintaining Holocene-like conditions(*7*). The absorption of latent heat during melting helps significantly slow down regional and global warming(*8*). The cryosphere changes significantly affect weather patterns and precipitation by impacting local evaporation and atmospheric water content(*115*), and the polar cryosphere changes also reduce temperature gradients between poles and equator. Worryingly, the cryosphere influences the thermohaline circulation (such as the North Atlantic Current and AMOC) by releasing meltwater into the ocean, which distributes heat and regulates climates globally(*116, 117*). Additionally, atmospheric ice also plays a crucial role in Earth's radiation balance and climate dynamics by reflecting incoming sunlight, influencing cloud formation and precipitation types(*118*). The cryosphere also provides cold conditions necessary for stratospheric clouds and ozone formation(*119*), and also provides various sources of aerosols (such as sea ice salt aerosols, dust, cryoconite particles, and volcanic eruptions in glacial regions)(*120, 121*). Last but not least, permafrost is a critical carbon reservoir with an estimated amount of more than all fossil fuel reserves together, which has played a significant role in regulating the Earth's carbon cycle and climate(*69, 122, 123*).

Cryo-ecological regulation

The cryosphere is further critical for Earth system resilience through its crucial role in supporting diverse ecosystems and sustaining ecological balance, especially in polar and alpine regions, by influencing habitat stability, biodiversity, and ecological interactions. Snow and ice-covered areas provide unique habitats for a variety of species that are highly adapted to cold climates, including animals, plants, and microorganisms(*124*, *125*). Especially, sea ice is essential for marine food webs in polar regions, because the algae that grow on the underside of sea ice are a primary food source for tiny organisms like zooplankton, which in turn are eaten by fish, that again feed seabirds, and larger mammals, such as seals, whales, and polar bears(*126*). The cryosphere also has habitat areas, especially for species that depend on ice and snow for breeding and feeding(*127*). The terrestrial cryosphere in higher altitudes and latitudes can also provide essential climate refuges for cold-adapted species that can't survive warmer temperatures(*128*). In tundra regions, permafrost stabilizes soil and stores organic matter, impacting soil structure and nutrient availability(*129*). The frozen ground and sea ice can stabilize and prevent the seashore from erosion by ocean waves in high-latitude coastal areas, thereby maintaining coastal ecosystem stability(*130*). The glacial erosion and erosive cryospheric freeze-thaw processes over mountainous regions provide important sources of material (particles and nutrients) for the formation of proluvial fans, oases, and plains ecosystems(*5*). The mountainous cryosphere can further regulate downstream river and wetland ecosystems by providing critical water sources, sediment, and nutrients(*4*, *130*).

Cryo-hydrological regulation

The cryosphere is an essential component of the global water cycle, storing and cycling water in frozen form. The land ice holds around 70% of the world's freshwater as a huge water storage system(*131*). Among them, the mountain glaciers, Greenland Ice Sheet, and Antarctic Ice Sheet contain approximately 0.16 million km^3, 2.9 million km^3 and 30 million km^3 of ice; equivalent to 32cm, 7.4 m, and 57.5 m of sea level rise if melted entirely(*30*, *31*, *132*). It is estimated that the melting of glaciers and ice sheets has dominated the global mean sea-level rise, contributing with ~1.6 mm $year^{-1}$ from 2006 to 2018(*91*). The melting of smaller mountain glaciers and ice caps dominated the cryosphere's contribution to global mean sea level rise during the 20th Century, but Greenland and Antarctica ice sheets now represent the dominant source(*133*). In contrast, permafrost holds about 1.5 million km^3 of ice(*134*), and snowmelt contributes ~19% of the global freshwater supply annually(*135*). Permafrost regions contain frozen groundwater, which limits groundwater flow and creates unique hydrological systems(*136*). Mountain glaciers and snow cover have a unique function of "peak shaving and valley filling"(*137*), which maintains the relative stability of river runoff on annual or seasonal scales through the accumulation of large volumes of frozen water during cold and/or humid seasons and their ablation during hot and/or drought seasons(*65*, *138*). Mountain snowpack is the primary source of freshwater supply for major rivers in cold regions and those with mountain headwaters in North and South America, Europe, and Asia(*139*).

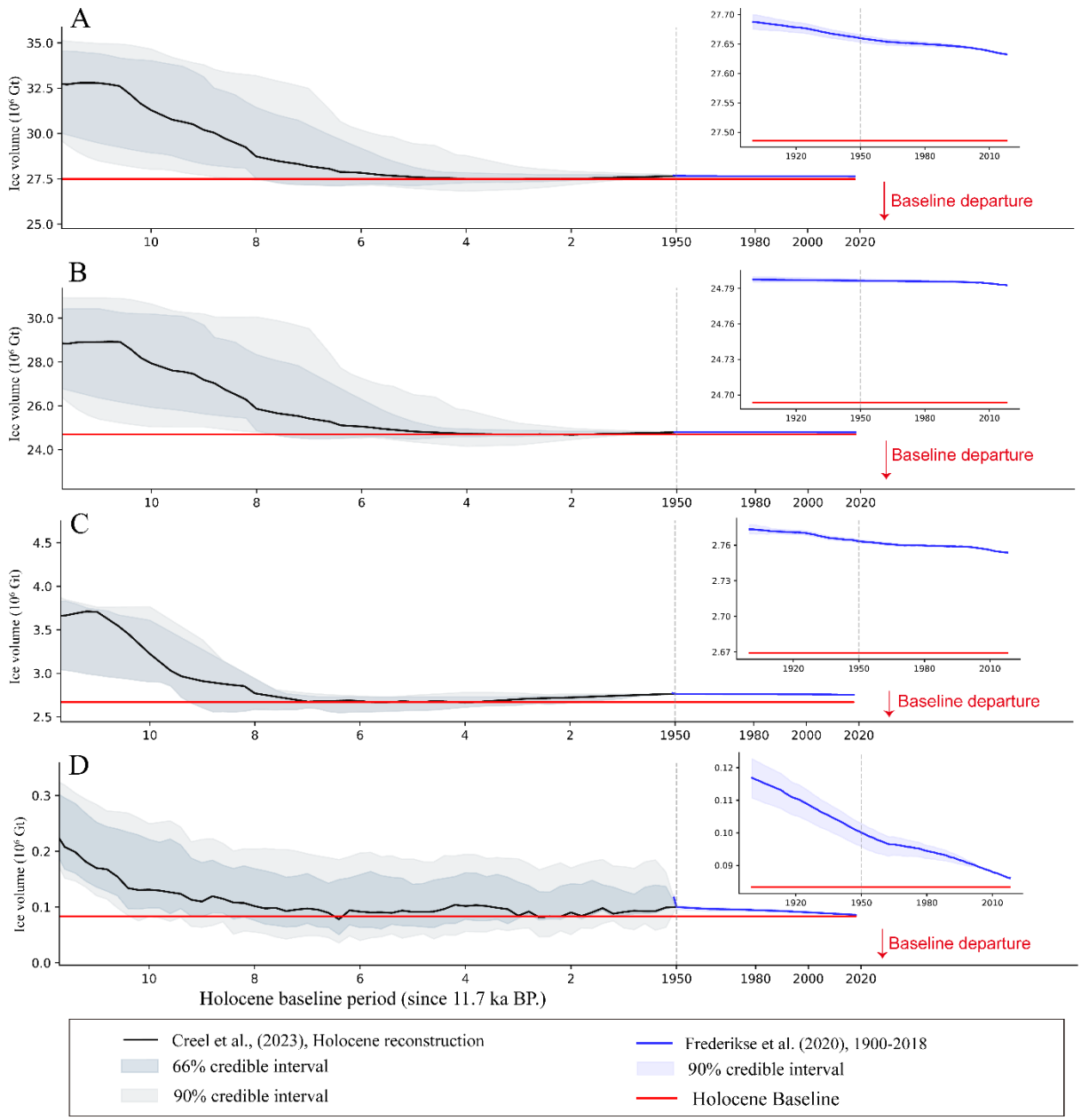


Fig. S1 Departure from the envelope of the Holocene baseline variability for land ice volume. **(A)** Global integrated land ice volume, i.e., the sum of ice volume of **(B)** Antarctica, **(C)** Greenland, and **(D)** Global mountains. The ice volume time series of land ice and components are reconstructed based on their estimated current volume and reconstructed variability of sea level equivalent(*28*, *29*). The ice volumes of global mountains, Greenland, and Antarctica were estimated to 0.088×10^6Gt, 2.756×10^6Gt, and 24.794×10^6Gt in 2010, respectively.

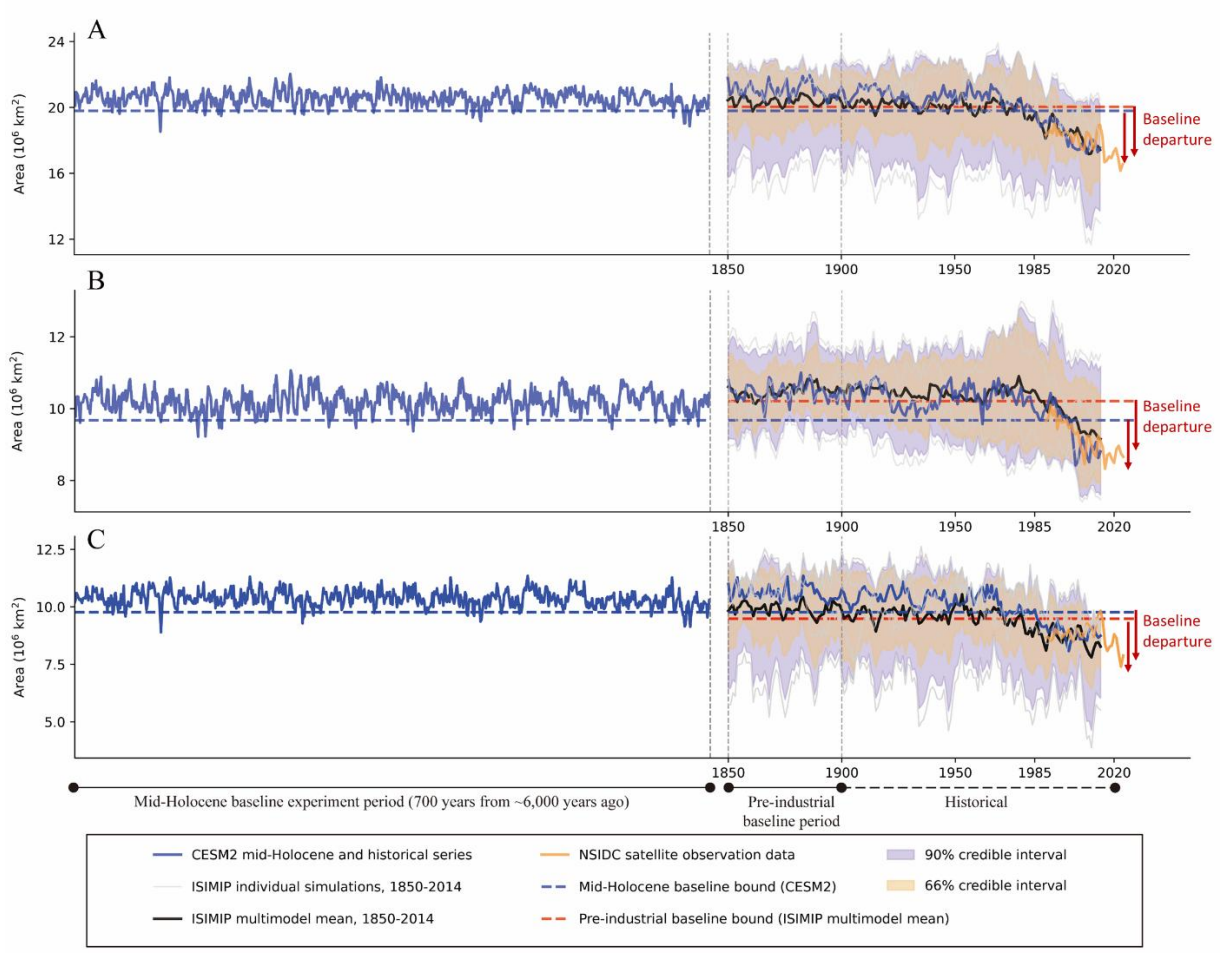


Fig. S2 Departure from the envelope of the mid-Holocene and pre-industrial baseline variability for annual-mean sea ice area. (A) Global sea ice, i.e., the sum of sea ice area of **(B)** Arctic sea ice and **(C)** Antarctic sea ice.

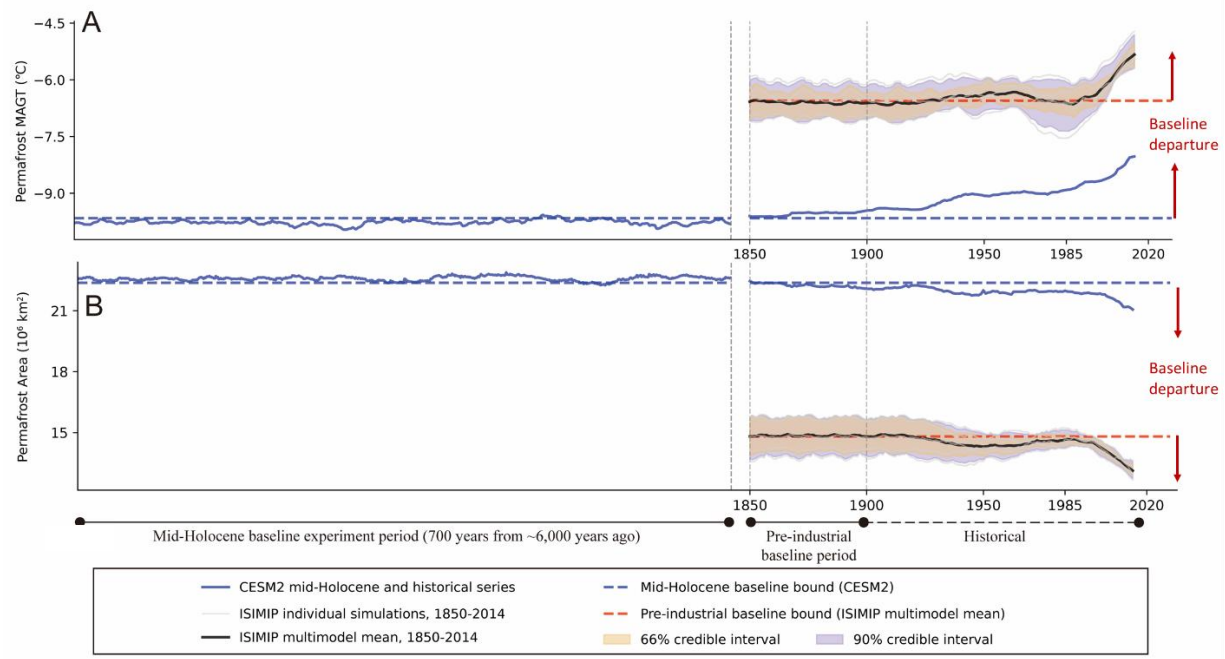


Fig. S3 Departure from the envelope of the mid-Holocene and pre-industrial baseline variability for global permafrost mean temperature (A) and associated permafrost area (B). Permafrost mean temperature refers to the mean annual ground temperature (MAGT) averaged over the global permafrost region. MAGT is the ground temperature at the depth of minimum amplitude for fluctuations in ground temperatures at the local scale, and the permafrost region is defined as the region that has a negative ground mean temperature. For each model, the permafrost mean temperature is calculated based on the maximum permafrost area during pre- industrial periods (1850-1899).

Table S1 Cryosphere components and associated functions for Earth resilience

Cryosphere elements	Functions	Descriptions	Importance	Implication for Earth resilience
Mountain glacier	Hydrological regulation	Lock up vast amounts of water; When they melt, the water flows into the ocean, causing sea-level rise; Acting as natural regulators of freshwater flow	***	Rapid melting rates make them major contributors to current sea-level rise; Sustain river flows during the dry season
	Climate regulation	Reflect solar radiation; Driving thermohaline circulation	***	Influence global and regional temperatures; Excess freshwater input from melting glaciers disrupts the circulation
	Ecological regulation	Sculpting landforms, provide unique habitats, deliver nutrients, and promote biodiversity; The freshwater input dilutes ocean salinity, particularly in regions where glacier-fed rivers meet the sea (e.g., the Gulf of Alaska, fjords in Greenland, and coastal zones)	**	Regional ecological regime shift and biodiversity loss' disrupt marine ecosystems, fisheries, and the ocean's capacity to store carbon and heat
Permafrost	Climate regulation	Massive carbon reservoir, storing an estimated 1,400–1,700 gigatons of carbon—almost twice the amount of carbon currently in the atmosphere	***	Influence the global carbon sink and climate stability
	Ecological regulation	Permafrost regions, such as the Arctic tundra, host unique ecosystems adapted to cold and frozen conditions; Influence on coastal ecosystems, ocean chemistry, and introduce freshwater into the ocean	***	Disrupt the stability of permafrost landscapes and biodiversity by altering water availability, soil stability, and nutrient cycles; Disrupt the stability of coast landscapes and marine ecosystems
	Hydrological regulation	Permafrost regions contain approximately 10,000–30,000 km^3 of ice in the form of ground ice, equivalent to about 3–4% of all freshwater on Earth; Regulates soil moisture, groundwater flow, and the formation of lakes, wetlands and perched water tables	***	Influence the stability of the global and regional freshwater cycle
Snow cover	Climate regulation	Snow reflects solar energy, cooling the Earth's surface and regulating temperature; Contributes mass of the cryosphere	***	Disrupt the stability of the cryosphere and climate system
	Hydrological regulation	Snow stores precipitation, releases it through spring and summer snowmelt, and regulates river discharge and soil moisture	***	Disrupt the stability of the global and regional water cycle
	Ecological regulation	Provides habitat for wildlife and influences plant growth, biodiversity, and seasonal rhythms; Influence marine ecosystems by affecting the salinity and temperature of ocean water, particularly in polar regions	***	Disrupt the stability of the global and regional ecosystem and biodiversity
	Climate	Reflects solar radiation, moderates	*	Influence local climate

Fresh water ice (lake and river ice)	regulation	temperatures, contributes to the regional climate		stability
	Runoff regulation	Regulates river flow, stores water, and affects seasonal discharge	*	Local hydrological regime shift
	Ecological regulation	Provides habitat, influences microbial and plant communities, and impacts nutrient cycling.	*	Local ecological regime shift
Ice sheets	Climate regulation	Reflects solar radiation, insulates the surface, stabilizes regional temperatures; Alters ocean salinity and impacts thermohaline circulation, influencing global climate	***	Disrupt the stability of the global and regional climate
	Hydrological regulation	Glaciers lock up vast amounts of water. When they melt, regulating regional water availability and causing global sea-level rise	***	Disrupt the stability of the global and regional water cycle
	Ecological regulation	Affects nutrient cycling, marine ecosystems, and global biogeochemical cycles	***	Disrupt the stability of global and regional ecology
Sea ice	Climate regulation	Reflects solar radiation, insulates ocean heat, affects polar vortex, jet stream; Drives the thermohaline circulation by regulating salinity and density	***	Disrupt the stability of regional and global climate and weather patterns
	Ecological regulation	Supports marine life and provides habitat for Arctic and Antarctic species	***	Disrupt the stability of regional ecology
Ice shelves and icebergs	Climate regulation	Provides thermal insulation, regulates heat exchange between ocean and atmosphere; affects thermohaline circulation by releasing freshwater and affecting the salinity and density of the ocean	**	Disrupt the stability of the regional climate
	Ecological regulation	Provides habitats for marine life, influences nutrient cycling and the marine food chain	*	Local ecological regime shift
	Hydrological regulation	Acts as a barrier to ice flow, preventing rapid sea-level rise. Its collapse accelerates ice flow into the ocean	*	Sea level rise
Atmosphere ice	Climate regulation	Reflects solar radiation (high albedo), moderates temperatures, and impacts global energy balance; Affects the formation of clouds, storms, and precipitation intensity (snow, hail, thunderstorms); Influences cloud formation, precipitation, and seasonal water storage (e.g., snowmelt).	***	Disrupt the stability of the global climate
	Atmospheric composition regulation	Affects chemical reactions in the atmosphere, including ozone depletion and aerosol formation.	**	Disrupt the stability of global atmospheric composition (ozone and aerosol)

Table S2. Cryosphere variables and their impacts on Earth system dynamics

Cryosphere elements	Variables	Descriptions	Units	Characteristics
Mountain glacier	Mass Balance and Equilibrium Line Altitude (ELA)	Measures the difference between the mass accumulation and ablation; The altitude at which accumulation and ablation (melting and sublimation) are balanced over a year.	Gt/yr or m w.e./yr for mass balance; m a.s.l. for ELA	A primary measure of glacier health and response to climate change
	Glacier Volume and thickness	The total ice volume of a glacier and the thickness of the ice across different points	km^3 or Gt for volume and m for thickness.	Contribution to water supply and sea-level rise. Glacier volume is a more direct indicator than glacier thickness
	Glacier area	The spatial extent of the glacier	km^2	Direct climate feedback, impacts on local hydrology and ecosystems
	Glacier velocity and flow rate	Measures the speed at which ice moves within the glacier, from the accumulation zone to the terminus	m/day or m/yr	Important for understanding glacier mass balance
	Meltwater	The volume of water generated by glacier melt and flowing into rivers, lakes, or oceans	m^3/s	Assessing freshwater availability for ecosystems and human use, as well as contributions to sea-level rise.
	Surface Albedo	The reflectivity of the glacier surface, which can vary due to snow cover, debris, or soot.	%	Lower albedo (less reflectivity) increases glacier melt by allowing more solar absorption
Permafrost	Permafrost Temperature	The temperature within the permafrost layer, often measured at various depths.	°C	Rising temperatures in permafrost indicate warming and potential thaw, leading to the release of greenhouse gasses and ground instability.
	Active Layer Thickness (ALT)	The thickness of the upper layer of soil that thaws and refreezes annually.	m	Increases in ALT indicate deeper seasonal thawing, which can affect vegetation, hydrology, leading to the release of greenhouse gases and ground instability.
	Permafrost Extent and Area	The geographical area covered by permafrost	km^2	Changes in permafrost extent reflect long-term warming trends and have implications for regional ecosystems and climate feedback.
	Soil moisture content in the active layer	The amount of water held in the active layer of permafrost, which can vary based on seasonal melting.	% or volumetric water content (m^3/m^3).	Soil moisture affects soil stability, vegetation, and the rates of organic matter decomposition, impacting carbon release.
	Ground Ice Content	The volume of ice within permafrost, present in forms such as ice wedges, pore ice, and massive ice.	% of soil volume or kg/m^3	High ground ice content makes permafrost highly susceptible to thaw and destabilization, impacting ecosystems and carbon

				release.
	Carbon and Methane Content	The amount of organic carbon and methane stored in permafrost soils.	GtC or methane (CH_4).	Thawing permafrost releases stored carbon as CO_2 and methane, potent greenhouse gases that amplify climate warming.
Snow cover	Snow Cover Extent (SCE)	The geographical area covered by snow at a given time.	km^2 or % of land area.	influence Earth's albedo and global energy balance, and provide a measure of seasonal climate patterns
	Snow Depth	The vertical thickness of the snow layer on the ground.	cm or m	Snow depth affects insulation of the ground below, impacting soil temperature, vegetation, and local wildlife
	Snow Water Equivalent (SWE)	The amount of water contained within the snowpack if it were melted	mm	SWE is crucial for water resource management, especially in regions dependent on snowmelt for water supply
	Snow Density	The mass of snow per unit volume, which varies based on snow age, compaction, and moisture content.	kg/m^3	Higher density indicates compaction and potential melt, influencing snow stability and water content.
	Albedo of Snow Surface	The reflectivity of snow, which changes with snow aging, impurities, and snow grain size.	%	High albedo reflects sunlight, keeping temperatures cooler, while lower albedo increases absorption and accelerates melting.
Ice sheets	Ice Sheet Thickness	The vertical depth of the ice sheet from the surface to the bedrock	m	Changes in thickness can indicate ice loss or gain, reflecting ice sheet stability and contributions to sea-level rise
	Ice Sheet Volume	The total ice volume of ice sheet	km^3 or Gt	Contribution to water supply and sea-level rise
	Ice Flow Velocity	The rate at which ice moves over the bedrock, particularly in areas like glaciers and ice streams within ice sheets.	m/yr	Increased ice flow can signal instability, often due to warming temperatures or lubrication from meltwater at the base.
	Surface Mass Balance (SMB)	The difference between ice gain (from snowfall) and ice loss (from melting and sublimation) on the surface.	Gt/yr or mm w.e./yr	A negative SMB indicates ice loss and contributes to sea-level rise, while a positive balance suggests ice growth.
	Subglacial Hydrology and Meltwater Production	The water produced at the ice sheet's base due to melting from geothermal heat or friction.	m^3/s or m w.e.	Meltwater can lubricate the base, increasing ice flow and contributing to ice loss.
	Ice Sheet Albedo	The reflectivity of the ice surface, influenced by snow cover, impurities, and surface melting.	%	Lower albedo (e.g., due to dust or soot) accelerates melting by absorbing more solar radiation.

Sea ice	Sea Ice Extent	The total area of the ocean covered by sea ice, often divided into regions of 15% or more ice concentration.	km^2	Changes in sea ice extent indicate seasonal and long-term shifts in polar climates and contribute to feedback loops in the climate system
	Sea Ice Thickness	The vertical depth of sea ice from the surface to the bottom.	m	Thickness affects the thermal insulation of the ocean and helps determine sea ice volume, impacting the energy exchange between the ocean and atmosphere
	Sea Ice Volume	The total volume of sea ice, calculated by combining thickness and extent.	km^3	Volume provides a complete measure of sea ice changes, reflecting both spatial extent and vertical structure, essential for understanding ice dynamics and climate impacts
	Ice Concentration	The proportion of an area covered by sea ice, typically given as a percentage.	%	Ice concentration affects surface reflectivity and the amount of solar radiation absorbed by the ocean, impacting regional temperatures.
	Sea Ice Albedo	The reflectivity of sea ice, which varies depending on snow cover, age, and ice type.	%	High albedo reflects solar radiation, cooling the region, while lower albedo absorbs heat, accelerating melting.

Table S3 Evaluating the suitability of control variables in the cryosphere.

Criteria	Control variable for each cryosphere sub-system				
	Land ice volume	Sea ice area	Snow cover area	Permafrost temperature	Atmosphere ice volume
1. Importance for Holocene-like Earth: Is the control variable critical for maintaining the Holocene-like conditions on Earth?	Major role in sea level, water supply, and climate and ecological stability	Strong influence on climate and polar biological feedbacks	Strong impact on planetary energy balance, and regional bio-physical feedbacks	Key in GHG release, Earth energy balance, landscape, and ecological stabilities	Impacts on radiative forcing and regional climate patterns
2. Human perturbation: Can the variable serve as a robust and comprehensive indicator of anthropogenic perturbation on critical cryosphere functions?	Driven by anthropogenic climate change and regional human disturbance, such as black carbon emission	Driven by anthropogenic warming and regional human disturbance, such as black carbon emission	Impacted by climate warming from human emissions	Sensitive to surface warming from human emissions and regional human disturbance, such as deforestation and infrastructure development	Not meaningfully perturbed by human activity
3. Universality and uniqueness: Is the variable able to directly or indirectly represent multiple components and dynamics of the cryosphere? Is the variable unique to the cryosphere	Broadly applicable and specific to the cryosphere; defining features of the Holocene-like interglacial Earth system state	Widely used and unique to the cryosphere	Widely used and unique to the cryosphere	Widely applicable and unique to frozen ground systems	Occurs globally, but not unique or critical to cryosphere
4. Measurability: can the status of the control variable be measured, tracked in time and monitored for both baseline and current conditions?	Measured reliably with satellite and field data, simulated and projected by land ice models	Well monitored by satellites; simulated and projected by sea ice models	Good observations by satellites and snow sensors, simulated and projected via Earth system models	Monitored by situ observation, simulated and projected via Earth system models	Observable via satellite and radar, but sparse data

Note: candidate control variables were assessed through literature review, expert elicitation, iterative discussion, and consensus-based workshops.

Table S4 Overview of sea ice data sources

Time period	data source	Variant	Resolution
Mid-Holocene	CESM2 experiment	r1i1p1f1	Monthly, 1°
Historical (1850-2014)	CESM2 output	r1i1p1f1	Monthly, 1°
Historical (1850-2014)	ISIMIP GFDL-ESM4 output	r1i1p1f1	Monthly, 1°
Historical (1850-2014)	ISIMIP UKESM1-0-LL output	r1i1p1f1	Monthly, 1°
Historical (1850-2014)	ISIMIP MPI-ESM1-2-HR output	r1i1p1f1	Monthly, 1°
Historical (1850-2014)	ISIMIP IPSL-CM6A-LR output	r1i1p1f1	Monthly, 1°

Table S5 Overview of permafrost mean temperature data sources

Time period	data source	Variant	Resolution	Depth (m)
Mid-Holocene	CESM2 experiment	r1i1p1f1	Monthly, 1.25°	0~42
Historical (1850-2014)	CESM2 output	r1i1p1f1	Monthly, 1.25°	0~42
Historical (1850-2014)	ELM-ECA forced by GFDL-ESM4	r1i1p1f1	Monthly, 0.5°	0~42
Historical (1850-2014)	ELM-ECA forced by IPSL-CM6A-LR	r1i1p1f1	Monthly, 0.5°	0~42
Historical (1850-2014)	ELM-ECA forced by MPI-ESM1-2-HR	r1i1p1f1	Monthly, 0.5°	0~42
Historical (1850-2014)	ELM-ECA forced by MRI-ESM2-0	r1i1p1f1	Monthly, 0.5°	0~42
Historical (1850-2014)	ELM-ECA forced by UKESM1-0-LL	r1i1p1f1	Monthly, 0.5°	0~42

Table S6 Overview of monthly snow area fraction data sources

Time period	data source	Variant
Mid-Holocene	CMIP6 CESM2 mid-Holocene experiment	r1i1p1f1
Historical (1850-2014)	CMIP6 CESM2	r1i1p1f1
Historical (1850-2014)	CMIP6 BCC-CSM2-MR	r1i1p1f1
Historical (1850-2014)	CMIP6 HadGEM3-GC31-MM	r1i1p1f3
Historical (1850-2014)	CMIP6 CESM2-FV2	r1i2p2f1
Historical (1850-2014)	CMIP6 CESM2-WACCM-FV2	r1i1p1f1
Historical (1850-2014)	CMIP6 NorESM2-MM	r1i1p1f1
Historical (1850-2014)	CMIP6 SNU.SAM0-UNICON	r1i1p1f1
Historical (1850-2014)	CMIP6 MPI-ESM1-2-HR	r1i1p1f1
Historical (1850-2014)	CMIP6 CESM2-WACCM	r1i1p1f1
Historical (1850-2014)	CMIP6 CMCC-CM2-HR4	r1i1p1f1
Historical (1850-2014)	CMIP6 CMCC-CM2-SR5	r1i1p1f1
Historical (1850-2014)	CMIP6 CMCC-ESM2	r1i1p1f1
Historical (1850-2014)	CMIP6 MRI-ESM2-0	r1i1p1f1
Historical (1850-2014)	CMIP6 TaiESM1	r1i1p1f1

Note: all Earth system models have a nominal 100 km resolution.

References and Notes

1. J. Rockström, W. Steffen, K. Noone, A. Persson, F. S. Chapin III, E. F. Lambin, T. M. Lenton, M. Scheffer, C. Folke, H. J. Schellnhuber, B. Nykvist, C. A. de Wit, T. Hughes, S. van der Leeuw, H. Rodhe, S. Sörlin, P. K. Snyder, R. Costanza, U. Svedin, M. Falkenmark, L. Karlberg, R. W. Corell, V. J. Fabry, J. Hansen, B. Walker, D. Liverman, K. Richardson, P. Crutzen, J. A. Foley, A safe operating space for humanity. *Nature* **461**, 472–475 (2009). doi:10.1038/461472a

2. W. Steffen, K. Richardsön, J. Rockström, S. E. Cornell, I. Fetzer, E. M. Bennett, R. Biggs, S. R. Carpenter, W. de Vries, C. A. de Wit, C. Folke, D. Gerten, J. Heinke, G. M. Mace, L. M. Persson, V. Ramanathan, B. Reyers, S. Sörlin, Planetary boundaries: Guiding human development on a changing planet. *Science* **347**, 1259855 (2015). doi:10.1126/science.1259855

3. C.-D. Xiao, S.-J. Wang, D.-H. Qin, A Preliminary study of cryosphere service function and value evaluation. *Adv. Clim. Chang. Res.* **6**, 181–187 (2015). doi:10.1016/j.accre.2015.11.004

4. A. M. Milner, K. Khamis, T. J. Battin, J. E. Brittain, N. E. Barrand, L. Füreder, S. Cauvy-Fraunié, G. M. Gíslason, D. Jacobsen, D. M. Hannah, A. J. Hodson, E. Hood, V. Lencioni, J. S. Ólafsson, C. T. Robinson, M. Tranter, L. E. Brown, Glacier shrinkage driving global changes in downstream systems. *Proc. Natl. Acad. Sci. U.S.A.* **114**, 9770–9778 (2017). doi:10.1073/pnas.1619807114

5. B. Su, C. Xiao, D. Chen, D. Qin, Y. Ding, Cryosphere services and human well-being. *Sustainability* **11**, 4365 (2019). doi:10.3390/su11164365

6. D. Qin, Y. Ding, C. Xiao, S. Kang, J. Ren, J. Yang, S. Zhang, Cryospheric Science: Research framework and disciplinary system. *Natl. Sci. Rev.* **5**, 255–268 (2018). doi:10.1093/nsr/nwx108

7. V. Melnikov, V. Gennadinik, M. Kulmala, H. K. Lappalainen, T. Petäjä, S. Zilitinkevich, Cryosphere: A kingdom of anomalies and diversity. *Atmos. Chem. Phys.* **18**, 6535–6542 (2018). doi:10.5194/acp-18-6535-2018

8. L. A. Hirose, A. Abe-Ouchi, W.-L. Chan, R. O'ishi, M. Yoshimori, T. Obase, Arctic warming suppressed by remnant glacial ice sheets in past interglacials. *Geophys. Res. Lett.* **52**, e2024GL111798 (2025). doi:10.1029/2024GL111798

9. J. Rockström, L. Kotzé, S. Milutinović, F. Biermann, V. Brovkin, J. Donges, J. Ebbesson, D. French, J. Gupta, R. Kim, T. Lenton, D. Lenzi, N. Nakicenovic, B. Neumann, F. Schuppert, R. Winkelmann, K. Bosselmann, C. Folke, W. Lucht, D. Schlosberg, K. Richardson, W. Steffen, The planetary commons: A new paradigm for safeguarding Earth-regulating systems in the Anthropocene. *Proc. Natl. Acad. Sci. U. S. A.* **121**, e2301531121 (2024). doi:10.1073/pnas.2301531121

10. B. Marzeion, J. G. Cogley, K. Richter, D. Parkes, Glaciers. Attribution of global glacier mass loss to anthropogenic and natural causes. *Science* **345**, 919–921 (2014). doi:10.1126/science.1254702 25123485

11. Intergovernmental Panel on Climate Change, *Climate Change 2021 - The Physical Science Basis* (Cambridge Univ. Press, Cambridge, UK, 2023).

12. J. R. McConnell, R. Edwards, G. L. Kok, M. G. Flanner, C. S. Zender, E. S. Saltzman, J. R. Banta, D. R. Pasteris, M. M. Carter, J. D. W. Kahl, 20th-century industrial black carbon emissions altered Arctic climate forcing. *Science* **317**, 1381–1384 (2007). doi:10.1126/science.1144856 17690261

13. Z. Zhang, F. Chen, H. Lin, C. Wang, X. Liu, M. Wang, J. Luo, Satellite observations characterize the impacts of climate change and human activities on permafrost along Qinghai–Tibet Railway. *Innov. Geosci.* **3**, 100127 (2025). doi:10.59717/j.xinn-geo.2024.100127

14. C. Xiao, B. Su, X. Wang, D. Qin, Cascading risks to the deterioration in cryospheric functions and services. *Chin. Sci. Bull.* **64**, 1975–1984 (2019). doi:10.1360/N972018-01314

15. T. M. Lenton, H. Held, E. Kriegler, J. W. Hall, W. Lucht, S. Rahmstorf, H. J. Schellnhuber, Tipping elements in the Earth's climate system. *Proc. Natl. Acad. Sci. U.S.A.* **105**, 1786–1793 (2008). doi:10.1073/pnas.0705414105 18258748

16. V. Dakos, M. Scheffer, E. H. van Nes, V. Brovkin, V. Petoukhov, H. Held, Slowing down as an early warning signal for abrupt climate change. *Proc. Natl. Acad. Sci. U.S.A.* **105**, 14308–14312 (2008). doi:10.1073/pnas.0802430105

17. D. I. Armstrong McKay, A. Staal, J. F. Abrams, R. Winkelmann, B. Sakschewski, S. Loriani, I. Fetzer, S. E. Cornell, J. Rockström, T. M. Lenton, Exceeding 1.5°C global warming could trigger multiple climate tipping points. *Science* **377**, eabn7950 (2022). doi:10.1126/science.abn7950 36074831

18. S. Wang, A. Foster, E. A. Lenz, J. D. Kessler, J. C. Stroeve, L. O. Anderson, M. Turetsky, R. Betts, S. Zou, W. Liu, W. R. Boos, Z. Hausfather, Mechanisms and impacts of earth system tipping elements. *Rev. Geophys.* **61**, e2021RG000757 (2023). doi:10.1029/2021RG000757

19. T. Liu, D. Chen, L. Yang, J. Meng, Z. Wang, J. Ludescher, J. Fan, S. Yang, D. Chen, J. Kurths, X. Chen, S. Havlin, H. J. Schellnhuber, Teleconnections among tipping elements in the Earth system. *Nat. Clim. Chang.* **13**, 67–74 (2023). doi:10.1038/s41558-022-01558-4

20. K. Richardson, W. Steffen, W. Lucht, J. Bendtsen, S. E. Cornell, J. F. Donges, M. Drüke, I. Fetzer, G. Bala, W. von Bloh, G. Feulner, S. Fiedler, D. Gerten, T. Gleeson, M. Hofmann, W. Huiskamp, M. Kummu, C. Mohan, D. Nogués-Bravo, S. Petri, M. Porkka, S. Rahmstorf, S. Schaphoff, K. Thonicke, A. Tobian, V. Virkki, L. Wang-Erlandsson, L. Weber, J. Rockström, Earth beyond six of nine planetary boundaries. *Sci. Adv.* **9**, eadh2458 (2023). doi:10.1126/sciadv.adh2458 37703365

21. J. Rockström, J. F. Donges, I. Fetzer, M. A. Martin, L. Wang-Erlandsson, K. Richardson, Planetary Boundaries guide humanity's future on Earth. *Nat. Rev. Earth Environ.* **5**, 773–788 (2024). doi:10.1038/s43017-024-00597-z

22. J. Rockström, W. Steffen, K. Noone, Å. Persson, F. S. Chapin Iii, E. Lambin, T. M. Lenton, M. Scheffer, C. Folke, H. J. Schellnhuber, B. Nykvist, C. A. de Wit, T. Hughes, S. van der Leeuw, H. Rodhe, S. Sörlin, P. K. Snyder, R. Costanza, U. Svedin, M. Falkenmark, L. Karlberg, R. W. Corell, V. J. Fabry, J. Hansen, B. Walker, D. Liverman, K. Richardson, P. Crutzen, J. Foley,

Planetary boundaries: Exploring the safe operating space for humanity. *Ecol. Soc.* **14**, 32 (2009). doi:10.5751/ES-03180-140232

23. Z. Liu, J. Zhu, Y. Rosenthal, X. Zhang, B. L. Otto-Bliesner, A. Timmermann, R. S. Smith, G. Lohmann, W. Zheng, O. Elison Timm, The Holocene temperature conundrum. *Proc. Natl. Acad. Sci. U.S.A.* **111**, E3501–E3505 (2014). doi:10.1073/pnas.1407229111 25114253

24. D. S. Kaufman, E. Broadman, Revisiting the Holocene global temperature conundrum. *Nature* **614**, 425–435 (2023). doi:10.1038/s41586-022-05536-w 36792734

25. S. A. Marcott, J. D. Shakun, P. U. Clark, A. C. Mix, A reconstruction of regional and global temperature for the past 11,300 years. *Science* **339**, 1198–1201 (2013). doi:10.1126/science.1228026 23471405

26. L. Wang-Erlandsson, A. Tobian, R. J. van der Ent, I. Fetzer, S. te Wierik, M. Porkka, A. Staal, F. Jaramillo, H. Dahlmann, C. Singh, P. Greve, D. Gerten, P. W. Keys, T. Gleeson, S. E. Cornell, W. Steffen, X. Bai, J. Rockström, A planetary boundary for green water. *Nat. Rev. Earth Environ.* **3**, 380–392 (2022). doi:10.1038/s43017-022-00287-8

27. M. Porkka, V. Virkki, L. Wang-Erlandsson, D. Gerten, T. Gleeson, C. Mohan, I. Fetzer, F. Jaramillo, A. Staal, S. te Wierik, A. Tobian, R. van der Ent, P. Döll, M. Flörke, S. N. Gosling, N. Hanasaki, Y. Satoh, H. Müller Schmied, N. Wanders, J. S. Famiglietti, J. Rockström, M. Kummu, Notable shifts beyond pre-industrial streamflow and soil moisture conditions transgress the planetary boundary for freshwater change. *Nat. Water* **2**, 262–273 (2024). doi:10.1038/s44221-024-00208-7

28. R. C. Creel, J. Austermann, R. E. Kopp, N. S. Khan, T. Albrecht, J. Kingslake, Global mean sea level likely higher than present during the holocene. *Nat. Commun.* **15**, 10731 (2024). doi:10.1038/s41467-024-54535-0

29. T. Frederikse, F. Landerer, L. Caron, S. Adhikari, D. Parkes, V. W. Humphrey, S. Dangendorf, P. Hogarth, L. Zanna, L. Cheng, Y.-H. Wu, The causes of sea-level rise since 1900. *Nature* **584**, 393–397 (2020). doi:10.1038/s41586-020-2591-3

30. D. Farinotti, M. Huss, J. J. Fürst, J. Landmann, H. Machguth, F. Maussion, A. Pandit, A consensus estimate for the ice thickness distribution of all glaciers on Earth. *Nat. Geosci.* **12**, 168–173 (2019). doi:10.1038/s41561-019-0300-3

31. M. Morlighem, C. N. Williams, E. Rignot, L. An, J. E. Arndt, J. L. Bamber, G. Catania, N. Chauché, J. A. Dowdeswell, B. Dorschel, I. Fenty, K. Hogan, I. Howat, A. Hubbard, M. Jakobsson, T. M. Jordan, K. K. Kjeldsen, R. Millan, L. Mayer, J. Mouginot, B. P. Y. Noël, C. O'Cofaigh, S. Palmer, S. Rysgaard, H. Seroussi, M. J. Siegert, P. Slabon, F. Straneo, M. R. van den Broeke, W. Weinrebe, M. Wood, K. B. Zinglersen, BedMachine v3: Complete bed topography and ocean bathymetry mapping of Greenland from multibeam echo sounding combined with mass conservation. *Geophys. Res. Lett.* **44**, 11051–11061 (2017). doi:10.1002/2017GL074954

32. P. Fretwell, H. D. Pritchard, D. G. Vaughan, J. L. Bamber, N. E. Barrand, R. Bell, C. Bianchi, R. G. Bingham, D. D. Blankenship, G. Casassa, G. Catania, D. Callens, H. Conway, A. J. Cook, H. F. J. Corr, D. Damaske, V. Damm, F. Ferraccioli, R. Forsberg, S. Fujita, Y. Gim, P. Gogineni, J. A. Griggs, R. C. A. Hindmarsh, P. Holmlund, J. W. Holt, R. W. Jacobel, A. Jenkins, W. Jokat, T. Jordan, E. C. King, J. Kohler, W. Krabill, M. Riger-Kusk, K. A. Langley, G. Leitchenkov, C. Leuschen, B. P. Luyendyk, K. Matsuoka, J. Mouginot, F. O. Nitsche, Y. Nogi, O. A. Nost, S. V. Popov, E. Rignot, D. M. Rippin, A. Rivera, J. Roberts, N. Ross, M. J. Siegert, A. M. Smith, D. Steinhage, M. Studinger, B. Sun, B. K. Tinto, B. C. Welch, D. Wilson, D. A. Young, C. Xiangbin, A. Zirizzotti, Bedmap2: Improved ice bed, surface and thickness datasets for Antarctica. *Cryosphere* **7**, 375–393 (2013). doi:10.5194/tc-7-375-2013.

33. W. Dobinski, Permafrost. *Earth Sci. Rev.* **108**, 158–169 (2011). doi:10.1016/j.earscirev.2011.06.007

34. T. M. Lenton, D. I. A. McKay, S. Loriani, J. F. Abrams, S. J. Lade, The global tipping points report 2025. (2025). https://pure.iiasa.ac.at/20918.

35. N. Wunderling, A. S. von der Heydt, Y. Aksenov, S. Barker, R. Bastiaansen, V. Brovkin, M. Brunetti, V. Couplet, T. Kleinen, C. H. Lear, J. Lohmann, R. M. Roman-Cuesta, S. Sinet, D. Swingedouw, R. Winkelmann, P. Anand, J. Barichivich, S. Bathiany, M. Baudena, J. T. Bruun,

C. M. Chiessi, H. K. Coxall, D. Docquier, J. F. Donges, S. K. J. Falkena, A. K. Klose, D. Obura, J. Rocha, S. Rynders, N. J. Steinert, M. Willeit, Climate tipping point interactions and cascades: a review. *Earth Syst. Dynam.* **15**, 41–74 (2024). doi:10.5194/esd-15-41-2024

36. J. E. Box, X. Fettweis, J. C. Stroeve, M. Tedesco, D. K. Hall, K. Steffen, Greenland ice sheet albedo feedback: thermodynamics and atmospheric drivers. *Cryosph. Discuss.* **6**, 821–839 (2012). doi:10.5194/tc-6-821-2012

37. J. M. Cook, A. J. Tedstone, C. Williamson, J. McCutcheon, A. J. Hodson, A. Dayal, M. Skiles, S. Hofer, R. Bryant, O. McAree, A. McGonigle, J. Ryan, A. M. Anesio, T. D. L. Irvine-Fynn, A. Hubbard, E. Hanna, M. Flanner, S. Mayanna, L. G. Benning, D. van As, M. Yallop, J. B. McQuaid, T. Gribbin, M. Tranter, Glacier algae accelerate melt rates on the south-western Greenland Ice Sheet. *Cryosphere* **14**, 309–330 (2020). doi:10.5194/tc-14-309-2020

38. K. Naegeli, M. Huss, M. Hoelzle, Change detection of bare-ice albedo in the Swiss Alps. *Cryosphere* **13**, 397–412 (2019). doi:10.5194/tc-13-397-2019

39. Y. Cho, H. Kim, R. J. Park, S.-W. Kim, Unprecedented East Siberian wildfires intensify Arctic snow darkening through enhanced poleward transport of black carbon. *Sci. Total Environ.* **961**, 178423 (2025). doi:10.1016/j.scitotenv.2025.178423

40. M.-H. Cho, R. J. Park, J. Yoon, Y. Choi, J. I. Jeong, L. Labzovskii, J. S. Fu, K. Huang, S.-J. Jeong, B.-M. Kim, A missing component of Arctic warming: black carbon from gas flaring. *Environ. Res. Lett.* **14**, 094011 (2019). doi:10.1088/1748-9326/ab374d

41. J. Oerlemans, Some basic experiments with a vertically-integrated ice sheet model. *Tellus* **33**, 1–11 (1981). doi:10.3402/tellusa.v33i1.10690

42. H. Bailey, A. Hubbard, Snow mass recharge of the Greenland ice sheet fueled by intense atmospheric river. *Geophys. Res. Lett.* **52, e2024GL110121** (2025). doi:10.1029/2024GL110121

43. J. Garbe, T. Albrecht, A. Levermann, J. F. Donges, R. Winkelmann, The hysteresis of the Antarctic Ice Sheet. *Nature* **585**, 538–544 (2020). doi:10.1038/s41586-020-2727-5

44. C. S. M. Turney, C. J. Fogwill, N. R. Golledge, N. P. McKay, E. van Sebille, R. T. Jones, D. Etheridge, M. Rubino, D. P. Thornton, S. M. Davies, C. B. Ramsey, Z. A. Thomas, M. I. Bird, N. C. Munksgaard, M. Kohno, J. Woodward, K. Winter, L. S. Weyrich, C. M. Rootes, H. Millman, P. G. Albert, A. Rivera, T. van Ommen, M. Curran, A. Moy, S. Rahmstorf, K. Kawamura, C.-D. Hillenbrand, M. E. Weber, C. J. Manning, J. Young, A. Cooper, Early Last Interglacial ocean warming drove substantial ice mass loss from Antarctica. *Proc. Natl. Acad. Sci. U.S.A.* **117**, 3996–4006 (2020). doi:10.1073/pnas.1902469117

45. J. N. Bassis, C. C. Walker, Upper and lower limits on the stability of calving glaciers from the yield strength envelope of ice. *Proc. R Soc. A* **468**, 913–931 (2012). doi:10.1098/rspa.2011.0422

46. A. K. Klose, V. Coulon, F. Pattyn, R. Winkelmann, The long-term sea-level commitment from Antarctica. *Cryosphere* **18**, 4463–4492 (2024). doi:10.5194/tc-18-4463-2024

47. K. Frieler, P. U. Clark, F. He, C. Buizert, R. Reese, S. R. M. Ligtenberg, M. R. van den Broeke, R. Winkelmann, A. Levermann, Consistent evidence of increasing Antarctic accumulation with warming. *Nat. Clim. Chang.* **5**, 348–352 (2015). doi:10.1038/nclimate2574

48. J. E. Box, N. Cressie, D. H. Bromwich, J.-H. Jung, M. van den Broeke, J. H. van Angelen, R. R. Forster, C. Miège, E. Mosley-Thompson, B. Vinther, J. R. McConnell, Greenland ice sheet mass balance reconstruction. Part I: Net snow accumulation (1600–2009). *J. Clim.* **26**, 3919–3934 (2013). doi:10.1175/JCLI-D-12-00373.1

49. B. Anderson, A. Mackintosh, Controls on mass balance sensitivity of maritime glaciers in the Southern Alps, New Zealand: The role of debris cover. *J. Geophys. Res.* **117**, F01003 (2012). doi:10.1029/2011JF002064

50. P. L. Whitehouse, N. Gomez, M. A. King, D. A. Wiens, Solid Earth change and the evolution of the Antarctic Ice Sheet. *Nat. Commun.* **10**, 503 (2019). doi:10.1038/s41467-018-08068-y 30700704

51. J. C. Rocha, G. Peterson, Ö. Bodin, S. Levin, Cascading regime shifts within and across scales. *Science* **362**, 1379–1383 (2018). doi:10.1126/science.aat785 30573623

52. M. Wang, J. E. Overland, A sea ice free summer Arctic within 30 years: An update from CMIP5 models. *Geophys. Res. Lett.* **39**, L18501 (2012). doi:10.1029/2012GL052868

53. T. J. W. Wagner, I. Eisenman, How climate model complexity influences sea ice stability. *J. Clim.* **28**, 3998–4014 (2015). doi:10.1175/JCLI-D-14-00654.1

54. N. J. Abram, A. Purich, M. H. England, F. S. McCormack, J. M. Strugnell, D. M. Bergstrom, T. R. Vance, T. Stål, B. Wienecke, P. Heil, E. W. Doddridge, J.-B. Sallée, T. J. Williams, A. M. Reading, A. Mackintosh, R. Reese, R. Winkelmann, A. K. Klose, P. W. Boyd, S. L. Chown, S. A. Robinson, Emerging evidence of abrupt changes in the Antarctic environment. *Nature* **644**, 621–633 (2025). doi:10.1038/s41586-025-09349-5 40836134

55. I. Eisenman, Geographic muting of changes in the Arctic sea ice cover. *Geophys. Res. Lett.* **37** (2010). doi:10.1029/2010GL043741

56. J. Selivanova, D. Iovino, F. Cocetta, Past and future of the Arctic sea ice in High-Resolution Model Intercomparison Project (HighResMIP) climate models. *Cryosphere* **18**, 2739–2763 (2024). doi:10.5194/tc-18-2739-2024

57. W. Hobbs, P. Spence, A. Meyer, S. Schroeter, A. D. Fraser, P. Reid, T. R. Tian, Z. Wang, G. Liniger, E. W. Doddridge, P. W. Boyd, Observational evidence for a regime shift in summer Antarctic sea ice. *J. Clim.* **37**, 2263–2275 (2024). doi:10.1175/JCLI-D-23-0479.1

58. E. W. Doddridge, W. R. Hobbs, M. Auger, P. W. Boyd, S. M. T. Chua, S. Cook, S. Corney, L. Emmerson, A. D. Fraser, P. Heil, N. Kelly, D. Lannuzel, X. Li, G. Liniger, R. A. Massom, A. Meyer, P. Reid, C. Southwell, P. Spence, A. Steketee, K. M. Swadling, N. Teder, B. Wienecke, P. Wongpan, K. Yamazaki, Impacts of Antarctic summer sea-ice extremes. *PNAS Nexus* **4**, pgaf164 (2025). doi:10.1093/pnasnexus/pgaf164 40599829

59. A. C. Y. Chan, M. England, J. A. Screen, T. J. Bracegirdle, E. W. Blockley, C. R. Holmes, Extreme Antarctic Sea Ice Loss facilitated by negative shift of Southern Annular Mode, *ESS Open Archive* (2025). doi:10.22541/essoar.174619838.82837699/v1

60. Z. Hou, L. Zhang, J. Peng, G. Forzieri, A. Jia, Z. Xiao, Y. Qu, J. Lin, D. Ji, Z. Zhu, X. Yao, S. Peng, L. Zhao, W. Fan, Z. Wu, H. Geng, Q. Wang, C. Zhou, S. Liu, L. Zhang, Radiative forcing reduced by early twenty-first century increase in land albedo. *Nature* **641**, 1162–1171 (2025). doi:10.1038/s41586-025-08987-z 40437163

61. M. G. Flanner, K. M. Shell, M. Barlage, D. K. Perovich, M. A. Tschudi, Radiative forcing and albedo feedback from the Northern Hemisphere cryosphere between 1979 and 2008. *Nat. Geosci.* **4**, 151–155 (2011). doi:10.1038/NGEO1062

62. X. Qu, A. Hall, On the persistent spread in snow-albedo feedback. *Clim. Dyn.* **42**, 69–81 (2014). doi:10.1007/s00382-013-1774-0

63. A. Detre, D. McGrath, E. Gagliano, R. Bonnell, R. Webb, H.-P. Marshall, D. Shean, Sentinel-1 SAR Estimates of snowmelt onset coincide with SNOTEL Soil moisture pulses across the Western United States. *Hydrol. Process.* **39**, e70341 (2025). doi:10.1002/hyp.70341

64. W. R. Berghuijs, R. A. Woods, M. Hrachowitz, A precipitation shift from snow towards rain leads to a decrease in streamflow. *Nat. Clim. Chang.* **4**, 583–586 (2014). doi:10.1038/nclimate2246

65. J. I. López-Moreno, J. W. Pomeroy, E. Alonso-González, E. Morán-Tejeda, J. Revuelto, Decoupling of warming mountain snowpacks from hydrological regimes. *Environ. Res. Lett.* **15**, 114006 (2020). doi:10.1088/1748-9326/abb55f

66. T. Kleinen, V. Brovkin, Pathway-dependent fate of permafrost region carbon. *Environ. Res. Lett.* **13**, 094001 (2018). doi:10.1088/1748-9326/aad824

67. K. Schaefer, H. Lantuit, V. E. Romanovsky, E. A. G. Schuur, R. Witt, The impact of the permafrost carbon feedback on global climate. *Environ. Res. Lett.* **9**, 085003 (2014). doi:10.1088/1748-9326/9/8/085003

68. A. Lindgren, P. Kuhry, M. Holloway, Z. Lu, G. Tanski, G. Hugelius, Massive losses and gains of northern land carbon stocks since the Last Glacial Maximum. *Sci. Adv.* **11**, eadt6231 (2025). doi:10.1126/sciadv.adt6231 40880482

69. K. R. Miner, M. R. Turetsky, E. Malina, A. Bartsch, J. Tamminen, A. D. McGuire, A. Fix, C. Sweeney, C. D. Elder, C. E. Miller, Permafrost carbon emissions in a changing Arctic. *Nat. Rev. Earth Environ.* **3**, 55–67 (2022). doi:10.1038/s43017-021-00230-3

70. J. Nitzbon, S. Westermann, M. Langer, L. C. P. Martin, J. Strauss, S. Laboor, J. Boike, Fast response of cold ice-rich permafrost in northeast Siberia to a warming climate. *Nat. Commun.* **11**, 2201 (2020). doi:10.1038/s41467-020-15725-8 32366820

71. M. R. Turetsky, B. W. Abbott, M. C. Jones, K. W. Anthony, D. Olefeldt, E. A. G. Schuur, G. Grosse, P. Kuhry, G. Hugelius, C. Koven, D. M. Lawrence, C. Gibson, A. B. K. Sannel, A. D. McGuire, Carbon release through abrupt permafrost thaw. *Nat. Geosci.* **13**, 138–143 (2020). doi:10.1038/s41561-019-0526-0

72. S. Wilkenskjeld, F. Miesner, P. P. Overduin, M. Puglini, V. Brovkin, Strong increase in thawing of subsea permafrost in the 22nd century caused by anthropogenic climate change. *Cryosphere* **16**, 1057–1069 (2022). doi:10.5194/tc-16-1057-2022

73. S.-W. Park, J.-H. Mun, H. Lee, N. J. Steinert, S.-I. An, J. Shin, J.-S. Kug, Continued permafrost ecosystem carbon loss under net-zero and negative emissions. *Sci. Adv.* **11**, eadn8819 (2025). doi:10.1126/sciadv.adn8819 39937912

74. T. M. Lenton, J. Rockström, O. Gaffney, S. Rahmstorf, K. Richardson, W. Steffen, H. J. Schellnhuber, Climate tipping points - too risky to bet against. *Nature* **575**, 592–595 (2019). doi:10.1038/d41586-019-03595-0 31776487

75. H. Zekollari, L. Schuster, F. Maussion, R. Hock, B. Marzeion, D. R. Rounce, L. Compagno, K. Fujita, M. Huss, M. James, P. D. A. Kraaijenbrink, W. H. Lipscomb, S. Minallah, M. Oberrauch, L. Van Tricht, N. Champollion, T. Edwards, D. Farinotti, W. Immerzeel, G. Leguy, A. Sakai, Glacier preservation doubled by limiting warming to 1.5°C versus 2.7°C. *Science* **388**, 979–983 (2025). doi:10.1126/science.adu4675 40440393

76. J. E. Box, A. Hubbard, D. B. Bahr, W. T. Colgan, X. Fettweis, K. D. Mankoff, A. Wehrlé, B. Noël, M. R. van den Broeke, B. Wouters, A. A. Bjørk, R. S. Fausto, Greenland ice sheet climate

disequilibrium and committed sea-level rise. *Nat. Clim. Chang.* **12**, 808–813 (2022). doi:10.1038/s41558-022-01441-2

77. R. M. DeConto, D. Pollard, R. B. Alley, I. Velicogna, E. Gasson, N. Gomez, S. Sadai, A. Condron, D. M. Gilford, E. L. Ashe, R. E. Kopp, D. Li, A. Dutton, The Paris Climate Agreement and future sea-level rise from Antarctica. *Nature* **593**, 83–89 (2021). doi:10.1038/s41586-021-03427-0 33953408

78. S. E. Chadburn, E. J. Burke, P. M. Cox, P. Friedlingstein, G. Hugelius, S. Westermann, An observation-based constraint on permafrost loss as a function of global warming. *Nat. Clim. Chang.* **7**, 340–344 (2017). doi:10.1038/nclimate3262

79. B. Wild, N. Shakhova, O. Dudarev, A. Ruban, D. Kosmach, V. Tumskoy, T. Tesi, H. Grimm, I. Nybom, F. Matsubara, H. Alexanderson, M. Jakobsson, A. Mazurov, I. Semiletov, Ö. Gustafsson, Organic matter composition and greenhouse gas production of thawing subsea permafrost in the Laptev Sea. *Nat. Commun.* **13**, 5057 (2022). doi:10.1038/s41467-022-32696-0

80. X. Pan, D. Chen, B. Pan, X. Huang, K. Yang, S. Piao, T. Zhou, Y. Dai, F. Chen, X. Li, Evolution and prospects of Earth system models: Challenges and opportunities. *Earth Sci. Rev.* **260**, 104986 (2025). doi:10.1016/j.earscirev.2024.104986

81. X. Li, M. Feng, Y. Ran, Y. Su, F. Liu, C. Huang, H. Shen, Q. Xiao, J. Su, S. Yuan, H. Guo, Big Data in Earth system science and progress towards a digital twin. *Nat. Rev. Earth Environ.* **4**, 319–332 (2023). doi:10.1038/s43017-023-00409-w

82. M. Tavoni, N. Bauer, L. Drouet, S. Fujimori, S. Paltsev, A. Pirani, K. Riahi, J. Rogelj, R. Schaeffer, D. van Vuuren, M. Weitzel, E. Kriegler, Implications of overshoot for climate mitigation strategies. *Nat. Clim. Chang.* **16**, 261–272 (2026). doi:10.1038/s41558-026-02563-7

83. P. D. L. Ritchie, J. J. Clarke, P. M. Cox, C. Huntingford, Overshooting tipping point thresholds in a changing climate. *Nature* **592**, 517–523 (2021). doi:10.1038/s41586-021-03263-2 33883733

84. J. Rockström, J. Gupta, D. Qin, S. J. Lade, J. F. Abrams, L. S. Andersen, D. I. Armstrong McKay, X. Bai, G. Bala, S. E. Bunn, D. Ciobanu, F. DeClerck, K. Ebi, L. Gifford, C. Gordon, S.

Hasan, N. Kanie, T. M. Lenton, S. Loriani, D. M. Liverman, A. Mohamed, N. Nakicenovic, D. Obura, D. Ospina, K. Prodani, C. Rammelt, B. Sakschewski, J. Scholtens, B. Stewart-Koster, T. Tharammal, D. van Vuuren, P. H. Verburg, R. Winkelmann, C. Zimm, E. M. Bennett, S. Bringezu, W. Broadgate, P. A. Green, L. Huang, L. Jacobson, C. Ndehedehe, S. Pedde, J. Rocha, M. Scheffer, L. Schulte-Uebbing, W. de Vries, C. Xiao, C. Xu, X. Xu, N. Zafra-Calvo, X. Zhang, Safe and just Earth system boundaries. *Nature* **619**, 102–111 (2023). doi:10.1038/s41586-023-06083-8

85. J. Gupta, X. Bai, D. M. Liverman, J. Rockström, D. Qin, B. Stewart-Koster, J. C. Rocha, L. Jacobson, J. F. Abrams, L. S. Andersen, D. I. Armstrong McKay, G. Bala, S. E. Bunn, D. Ciobanu, F. DeClerck, K. L. Ebi, L. Gifford, *C. Gordon*, S. Hasan, N. Kanie, T. M. Lenton, S. Loriani, A. Mohamed, N. Nakicenovic, D. Obura, D. Ospina, K. Prodani, C. Rammelt, B. Sakschewski, J. Scholtens, T. Tharammal, D. van Vuuren, P. H. Verburg, R. Winkelmann, C. Zimm, E. Bennett, A. Bjørn, S. Bringezu, W. J. Broadgate, H. Bulkeley, B. Crona, P. A. Green, H. Hoff, L. Huang, M. Hurlbert, C. Y. A. Inoue, Ş. Kılkış, S. J. Lade, J. Liu, I. Nadeem, C. Ndehedehe, C. Okereke, I. M. Otto, S. Pedde, L. Pereira, L. Schulte-Uebbing, J. D. Tàbara, W. de Vries, G. Whiteman, C. Xiao, X. Xu, N. Zafra-Calvo, X. Zhang, P. Fezzigna, G. Gentile, A just world on a safe planet: a Lancet Planetary Health-Earth Commission report on Earth-system boundaries, translations, and transformations. *Lancet Planet. Health* **8**, e813–e873 (2024). doi:10.1016/S2542-5196(24)00042-1

86. J. Gupta, D. Liverman, K. Prodani, P. Aldunce, X. Bai, W. Broadgate, D. Ciobanu, L. Gifford, *C. Gordon*, M. Hurlbert, C. Y. A. Inoue, L. Jacobson, N. Kanie, S. J. Lade, T. M. Lenton, D. Obura, C. Okereke, I. M. Otto, L. Pereira, J. Rockström, J. Scholtens, J. Rocha, B. Stewart-Koster, J. David Tàbara, C. Rammelt, P. H. Verburg, Earth system justice needed to identify and live within Earth system boundaries. *Nat. Sustain.* **6**, 630–638 (2023). doi:10.1038/s41893-023-01064-1

87. B. Su, C. Xiao, D. Chen, X. Ying, Y. Huang, R. Guo, H. Zhao, A. Chen, Y. Che, Mismatch between the population and meltwater changes creates opportunities and risks for global glacier-fed basins. *Science Bulletin* **67**, 9–12 (2022). doi:10.1016/j.scib.2021.07.027

88. X. Bai, S. Hasan, L. S. Andersen, A. Bjørn, Ş. Kilkiş, D. Ospina, J. Liu, S. E. Cornell, O. Sabag Muñoz, A. de Bremond, B. Crona, F. DeClerck, J. Gupta, H. Hoff, N. Nakicenovic, D. Obura, G. Whiteman, W. Broadgate, S. J. Lade, J. Rocha, J. Rockström, B. Stewart-Koster, D. van Vuuren, C. Zimm, Translating Earth system boundaries for cities and businesses. *Nat. Sustain.* **7**, 108–119 (2024). doi:10.1038/s41893-023-01255-w

89. B. Su, J. Rockström, D. Chen, I. Fetzer, H. Feng, G. Hugelius, R. Winkelmann, A. V. Norström, C. Xiao, E. Hanna, K. Alverson, J. E. Box, D. Qin, M. Sommerkorn, L. M. Andreassen, P. Heil, T. Yao, K. Richardson, S. J. Lade, X. Bai, J. Gupta, B. Stewart-Koster, Z. Zheng, J. Pomeroy, A. Mackintosh, T. OKI, A. Mukherji, M. Jackson, J. C. Rocha, J. Donges, L. Wang-Erlandsson, SOS-Cryo (Version v1.0.0), computer software, Zenodo (2026); https://doi.org/10.5281/zenodo.22992170.

90. T. Gleeson, L. Wang-Erlandsson, S. C. Zipper, M. Porkka, F. Jaramillo, D. Gerten, I. Fetzer, S. E. Cornell, L. Piemontese, L. J. Gordon, J. Rockström, T. Oki, M. Sivapalan, Y. Wada, K. A. Brauman, M. Flörke, M. F. P. Bierkens, B. Lehner, P. Keys, M. Kummu, T. Wagener, S. Dadson, T. J. Troy, W. Steffen, M. Falkenmark, J. S. Famiglietti, The water planetary boundary: Interrogation and revision. *One Earth* **2**, 223–234 (2020). doi:10.31223/osf.io/swhma

91. Intergovernmental Panel on Climate Change (IPCC), *The Ocean and Cryosphere in a Changing Climate: Special Report of the Intergovernmental Panel on Climate Change* (Cambridge Univ. Press, 2022).

92. L. Mudryk, M. Santolaria-Otín, G. Krinner, M. Ménégoz, C. Derksen, C. Brutel-Vuilmet, M. Brady, R. Essery, Historical Northern Hemisphere snow cover trends and projected changes in the CMIP6 multi-model ensemble. *Cryosphere* **14**, 2495–2514 (2020). doi:10.5194/tc-14-2495-2020

93. E. A. G. Schuur, A. D. McGuire, C. Schädel, G. Grosse, J. W. Harden, D. J. Hayes, G. Hugelius, C. D. Koven, P. Kuhry, D. M. Lawrence, S. M. Natali, D. Olefeldt, V. E. Romanovsky, K. Schaefer, M. R. Turetsky, C. C. Treat, J. E. Vonk, Climate change and the permafrost carbon feedback. *Nature* **520**, 171–179 (2015). doi:10.1038/nature14338 25855454

94. J. L. Bamber, R. M. Westaway, B. Marzeion, B. Wouters, The land ice contribution to sea level during the satellite era. *Environ. Res. Lett.* **13**, 063008 (2018). doi:10.1088/1748-9326/aac2f0

95. T. L. Edwards, S. Nowicki, B. Marzeion, R. Hock, H. Goelzer, H. Seroussi, N. C. Jourdain, D. A. Slater, F. E. Turner, C. J. Smith, C. M. McKenna, E. Simon, A. Abe-Ouchi, J. M. Gregory, E. Larour, W. H. Lipscomb, A. J. Payne, A. Shepherd, C. Agosta, P. Alexander, T. Albrecht, B. Anderson, X. Asay-Davis, A. Aschwanden, A. Barthel, A. Bliss, R. Calov, C. Chambers, N. Champollion, Y. Choi, R. Cullather, J. Cuzzone, C. Dumas, D. Felikson, X. Fettweis, K. Fujita, B. K. Galton-Fenzi, R. Gladstone, N. R. Golledge, R. Greve, T. Hattermann, M. J. Hoffman, A. Humbert, M. Huss, P. Huybrechts, W. Immerzeel, T. Kleiner, P. Kraaijenbrink, S. Le Clec'h, V. Lee, G. R. Leguy, C. M. Little, D. P. Lowry, J.-H. Malles, D. F. Martin, F. Maussion, M. Morlighem, J. F. O'Neill, I. Nias, F. Pattyn, T. Pelle, S. F. Price, A. Quiquet, V. Radić, R. Reese, D. R. Rounce, M. Rückamp, A. Sakai, C. Shafer, N.-J. Schlegel, S. Shannon, R. S. Smith, F. Straneo, S. Sun, L. Tarasov, L. D. Trusel, J. Van Breedam, R. van de Wal, M. van den Broeke, R. Winkelmann, H. Zekollari, C. Zhao, T. Zhang, T. Zwinger, Projected land ice contributions to twenty-first-century sea level rise. *Nature* **593**, 74–82 (2021). doi:10.1038/s41586-021-03302-y 33953415

96. H.-S. Park, S.-J. Kim, K.-H. Seo, A. L. Stewart, S.-Y. Kim, S.-W. Son, The impact of Arctic sea ice loss on mid-Holocene climate. *Nat. Commun.* **9**, 4571 (2018). doi:10.1038/s41467-018-07068-2

97. Y. Liu, D. Jiang, Mid-Holocene permafrost: Results from CMIP5 simulations. *J. Geophys. Res Atmos.* **121**, 221–240 (2016). doi:10.1002/2015JD023837

98. B. Marzeion, P. W. Leclercq, J. G. Cogley, A. H. Jarosch, Brief Communication: Global reconstructions of glacier mass change during the 20th century are consistent. *Cryosphere* **9**, 2399–2404 (2015). doi:10.5194/tc-9-2399-2015

99. M. Zemp, M. Huss, E. Thibert, N. Eckert, R. McNabb, J. Huber, M. Barandun, H. Machguth, S. U. Nussbaumer, I. Gärtner-Roer, L. Thomson, F. Paul, F. Maussion, S. Kutuzov, J. G. Cogley, Global glacier mass changes and their contributions to sea-level rise from 1961 to 2016. *Nature* **568**, 382–386 (2019). doi:10.1038/s41586-019-1071-0

100. K. K. Kjeldsen, N. J. Korsgaard, A. A. Bjørk, S. A. Khan, J. E. Box, S. Funder, N. K. Larsen, J. L. Bamber, W. Colgan, M. van den Broeke, M.-L. Siggaard-Andersen, C. Nuth, A. Schomacker, C. S. Andresen, E. Willerslev, K. H. Kjær, Spatial and temporal distribution of mass loss from the Greenland Ice Sheet since AD 1900. *Nature* **528**, 396–400 (2015). doi:10.1038/nature16183 26672555

101. J. Mouginot, E. Rignot, A. A. Bjørk, M. van den Broeke, R. Millan, M. Morlighem, B. Noël, B. Scheuchl, M. Wood, Forty-six years of Greenland Ice Sheet mass balance from 1972 to 2018. *Proc. Natl. Acad. Sci. U.S.A.* **116**, 9239–9244 (2019). doi:10.1073/pnas.1904242116 31010924

102. S. Adhikari, L. Caron, B. Steinberger, J. T. Reager, K. K. Kjeldsen, B. Marzeion, E. Larour, E. R. Ivins, What drives 20th century polar motion? *Earth Planet. Sci. Lett.* **502**, 126–132 (2018). doi:10.1016/j.epsl.2018.08.059

103. The IMBIE team, Mass balance of the Antarctic Ice Sheet from 1992 to 2017. *Nature* **558**, 219–222 (2018). doi:10.1038/s41586-018-0179-y

104. M. D. Fowler, R. B. Neale, T. Waterman, D. M. Lawrence, P. A. Dirmeyer, V. E. Larson, M. Huang, J. S. Simon, J. Truesdale, N. W. Chaney, Assessing the atmospheric response to subgrid surface heterogeneity in the single-column Community Earth System Model, version 2 (CESM2). *J. Adv. Model. Earth Syst.* **16**, e2022MS003517 (2024). doi:10.1029/2022MS003517

105. V. Eyring, S. Bony, G. A. Meehl, C. A. Senior, B. Stevens, R. J. Stouffer, K. E. Taylor, Overview of the Coupled Model Intercomparison Project Phase 6 (CMIP6) experimental design and organization. *Geosci. Model Dev.* **9**, 1937–1958 (2016). doi:10.5194/gmd-9-1937-2016

106. D. Notz, SIMIP Community, Arctic sea ice in CMIP6. *Geophys. Res. Lett.* **47**, e2019GL086749 (2020). doi:10.1029/2019GL086749

107. J. Muñoz-Sabater, E. Dutra, A. Agustí-Panareda, C. Albergel, G. Arduini, G. Balsamo, S. Boussetta, M. Choulga, S. Harrigan, H. Hersbach, B. Martens, D. G. Miralles, M. Piles, N. J. Rodríguez-Fernández, E. Zsoter, C. Buontempo, J. N. Thépaut, ERA5-Land: a state-of-the-art

global reanalysis dataset for land applications. *Earth Syst. Sci. Data* **13**, 4349–4383 (2021). doi:10.5194/essd-13-4349-2021

108. E. J. Burke, Y. Zhang, G. Krinner, Evaluating permafrost physics in the Coupled Model Intercomparison Project 6 (CMIP6) models and their sensitivity to climate change. *Cryosphere* **14**, 3155–3174 (2020). doi:10.5194/tc-14-3155-2020

109. C. Schädel, T. Gasser, B. M. Rogers, R. Treharne, M. R. Turetsky, T. Smith, E. MacDonald, S. M. Natali, Permafrost and wildfire carbon emissions indicate need for additional action to keep Paris Agreement temperature goals within reach. *Commun. Earth Environ.* **7**, 306 (2026). doi:10.1038/s43247-026-03189-5

110. G. L. Stephens, D. O'Brien, P. J. Webster, P. Pilewski, S. Kato, J.-l. Li, The albedo of Earth. *Rev. Geophys.* **53**, 141–163 (2015). doi:10.1002/2014RG000449

111. H. F. Goessling, T. Rackow, T. Jung, Recent global temperature surge intensified by record-low planetary albedo. *Science* **387**, 68–73 (2025). doi:10.1126/science.adq7280 39636934

112. K. von Schuckmann, A. Minière, F. Gues, F. J. Cuesta-Valero, G. Kirchengast, S. Adusumilli, F. Straneo, M. Ablain, R. P. Allan, P. M. Barker, H. Beltrami, A. Blazquez, T. Boyer, L. Cheng, J. Church, D. Desbruyeres, H. Dolman, C. M. Domingues, A. García-García, D. Giglio, J. E. Gilson, M. Gorfer, L. Haimberger, M. Z. Hakuba, S. Hendricks, S. Hosoda, G. C. Johnson, R. Killick, B. King, N. Kolodziejczyk, A. Korosov, G. Krinner, M. Kuusela, F. W. Landerer, M. Langer, T. Lavergne, I. Lawrence, Y. Li, J. Lyman, F. Marti, B. Marzeion, M. Mayer, A. H. MacDougall, T. McDougall, D. P. Monselesan, J. Nitzbon, I. Otosaka, J. Peng, S. Purkey, D. Roemmich, K. Sato, K. Sato, A. Savita, A. Schweiger, A. Shepherd, S. I. Seneviratne, L. Simons, D. A. Slater, T. Slater, A. K. Steiner, T. Suga, T. Szekely, W. Thiery, M.-L. Timmermans, I. Vanderkelen, S. E. Wjiffels, T. Wu, M. Zemp, Heat stored in the Earth system 1960–2020: where does the energy go? *Earth Syst. Sci. Data* **15**, 1675–1709 (2023). doi:10.5194/essd-15-1675-2023

113. M. Sturm, D. K. Perovich, J. Holmgren, Thermal conductivity and heat transfer through the snow on the ice of the Beaufort Sea. *J. Geophys. Res.* **107**, 8043 (2002). doi:10.1029/2000JC000409

114. T. V. Callaghan, M. Johansson, J. Key, T. Prowse, M. Ananicheva, A. Klepikov, Feedbacks and interactions: From the arctic cryosphere to the climate system. *Ambio* **40**, 75–86 (2011). doi:10.1007/s13280-011-0215-8

115. T. Vihma, J. Screen, M. Tjernström, B. Newton, X. Zhang, V. Popova, C. Deser, M. Holland, T. Prowse, The atmospheric role in the Arctic water cycle: A review on processes, past and future changes, and their impacts. *J. Geophys. Res. Biogeosci.* **121**, 586–620 (2016). doi:10.1002/2015JG003132

116. F. Sévellec, A. V. Fedorov, W. Liu, Arctic sea-ice decline weakens the Atlantic Meridional Overturning Circulation. *Nat. Clim. Chang.* **7**, 604–610 (2017). doi:10.1175/JCLI-D-18-0231.1

117. Y.-C. Lee, W. Liu, A. V. Fedorov, N. Feldl, P. C. Taylor, Impacts of Atlantic meridional overturning circulation weakening on Arctic amplification. *Proc. Natl. Acad. Sci. U.S.A.* **121**, e2402322121 (2024). doi:10.1073/pnas.2402322121 39284066

118. T. Dou, C. Xiao, Y. Huang, H. Yue, W. Han, Estimation of the atmospheric ice content mass, spatial distribution, and long-term changes based on the ERA5 reanalysis. *Geophys. Res. Lett.* **47**, e2020GL088186 (2020). doi:10.1029/2020GL088186

119. P. B. Shepson, "Cryosphere-Atmosphere Interactions" in *Chemistry in the Cryosphere*, (WORLD SCIENTIFIC, 2022).

120. J. M. Jaeger, M. N. Koppes, The role of the cryosphere in source-to-sink systems. *Earth Sci. Rev.* **153**, 43–76 (2016). doi:10.1016/j.earscirev.2015.09.011

121. B. Edwards, W. Kochtitzky, S. Battersby, Global mapping of future glaciovolcanism. *Glob. Planet. Change* **195**, 103356 (2020). doi:10.1016/j.gloplacha.2020.103356

122. S. A. Zimov, E. A. G. Schuur, F. S. Chapin 3rd, Climate change. Permafrost and the global carbon budget. *Science* **312**, 1612–1613 (2006). doi:10.1126/science.1128908 16778046

123. E. Hood, T. J. Battin, J. Fellman, S. O'Neel, R. G. M. Spencer, Storage and release of organic carbon from glaciers and ice sheets. *Nat. Geosci.* **8**, 91–96 (2015). doi:10.1038/ngeo2331

124. T. V. Callaghan, L. O. Björn, Y. Chernov, T. Chapin, T. R. Christensen, B. Huntley, R. A. Ims, M. Johansson, D. Jolly, S. Jonasson, N. Matveyeva, N. Panikov, W. Oechel, G. Shaver, J. Elster, H. Henttonen, K. Laine, K. Taulavuori, E. Taulavuori, C. Zöckler, Biodiversity, distributions and adaptations of Arctic species in the context of environmental change. *Ambio* **33**, 404–417 (2004). doi:10.1579/0044-7447-33.7.404 15573569

125. L. Maccario, L. Sanguino, T. M. Vogel, C. Larose, Snow and ice ecosystems: not so extreme. *Res. Microbiol.* **166**, 782–795 (2015). doi:10.1016/j.resmic.2015.09.002 26408452

126. M. A. Moline, N. J. Karnovsky, Z. Brown, G. J. Divoky, T. K. Frazer, C. A. Jacoby, J. J. Torres, W. R. Fraser, High latitude changes in ice dynamics and their impact on polar marine ecosystems. *Ann. N. Y. Acad. Sci.* **1134**, 267–319 (2008). doi:10.1196/annals.1439.010 18566098

127. W. F. Vincent, T. V. Callaghan, D. Dahl-Jensen, M. Johansson, K. M. Kovacs, C. Michel, T. Prowse, J. D. Reist, M. Sharp, Ecological implications of changes in the arctic cryosphere. *Ambio* **40**, 87–99 (2011). doi:10.1007/s13280-011-0218-5

128. W. F. Vincent, M. Lemay, M. Allard, Arctic permafrost landscapes in transition: towards an integrated Earth system approach. *Arct. Sci.* **3**, 39–64 (2017). doi:10.1139/AS-2016-0027

129. E. C. Geyman, M. M. Douglas, J.-P. Avouac, M. P. Lamb, Permafrost slows Arctic riverbank erosion. *Nature* **634**, 359–365 (2024). doi:10.1038/s41586-024-07978-w

130. M. Carey, O. C. Molden, M. B. Rasmussen, M. Jackson, A. W. Nolin, B. G. Mark, Impacts of glacier recession and declining meltwater on mountain societies. *Ann. Am. Assoc. Geogr.* **107**, 350–359 (2017). doi:10.1080/24694452.2016.1243039

131. G. L. Stephens, J. M. Slingo, E. Rignot, J. T. Reager, M. Z. Hakuba, P. J. Durack, J. Worden, R. Rocca, Earth's water reservoirs in a changing climate. *Proc. Math. Phys. Eng. Sci.* **476**, 20190458 (2020). DOI:10.1098/rspa.2019.0458 32398926

132. M. Morlighem, E. Rignot, T. Binder, D. Blankenship, R. Drews, G. Eagles, O. Eisen, F. Ferraccioli, R. Forsberg, P. Fretwell, V. Goel, J. S. Greenbaum, H. Gudmundsson, J. Guo, V. Helm, C. Hofstede, I. Howat, A. Humbert, W. Jokat, N. B. Karlsson, W. S. Lee, K. Matsuoka, R. Millan, J. Mouginot, J. Paden, F. Pattyn, J. Roberts, S. Rosier, A. Ruppel, H. Seroussi, E. C. Smith, D. Steinhage, B. Sun, M. R. van den Broeke, T. D. van Ommen, M. van Wessem, D. A. Young, Deep glacial troughs and stabilizing ridges unveiled beneath the margins of the Antarctic ice sheet. *Nat. Geosci.* **13**, 132–137 (2020). doi:10.1038/s41561-019-0510-8

133. C. R. Stokes, J. L. Bamber, A. Dutton, R. M. DeConto, Warming of +1.5 °C is too high for polar ice sheets. *Commun. Earth Environ.* **6**, 351 (2025). doi:10.1038/s43247-025-02299-w 40406387

134. T. Zhang, R. G. Barry, K. Knowles, J. A. Heginbottom, J. Brown, Statistics and characteristics of permafrost and ground-ice distribution in the Northern Hemisphere. *Polar Geogr.* **31**, 47–68 (2008). doi:10.1080/10889370802175895

135. J. Pulliainen, K. Luojus, C. Derksen, L. Mudryk, J. Lemmetyinen, M. Salminen, J. Ikonen, M. Takala, J. Cohen, T. Smolander, J. Norberg, Patterns and trends of Northern Hemisphere snow mass from 1980 to 2018. *Nature* **581**, 294–298 (2020). doi:10.1038/s41586-020-2258-0 32433620

136. J. M. McKenzie, C. I. Voss, Permafrost thaw in a nested groundwater-flow system. *Hydrogeol. J.* **21**, 299–316 (2013). doi:10.1007/s10040-012-0942-3

137. H. D. Pritchard, Asia's shrinking glaciers protect large populations from drought stress. *Nature* **569**, 649–654 (2019). doi:10.1038/s41586-019-1240-1 31142854

138. M. Huss, B. Bookhagen, C. Huggel, D. Jacobsen, R. S. Bradley, J. J. Clague, M. Vuille, W. Buytaert, D. R. Cayan, G. Greenwood, B. G. Mark, A. M. Milner, R. Weingartner, M. Winder,

Toward mountains without permanent snow and ice. *Earths Future* **5**, 418–435 (2017). doi:10.1002/2016EF000514

139. J. S. Mankin, D. Viviroli, D. Singh, A. Y. Hoekstra, N. S. Diffenbaugh, The potential for snow to supply human water demand in the present and future. *Environ. Res. Lett.* **10**, 114016 (2015). doi:10.1088/1748-9326/10/11/114016